International Symposium
On Turbulence and Shear Flow
Phenomena (TSFP-9)
June 30 - July 3, 2015 *Melbourne, Australia*

BOUNDARY LAYER STRUCTURE IN TURBULENT RAYLEIGH-BÉNARD CONVECTION IN AIR

Ronald du Puits
Institute of Thermodynamics and Fluid Mechanics...
Technische Universitaet Ilmenau
POB 100 565, 98684 Ilmenau, Germany
email: ronald.dupuits@tu-ilmenau.de

Christian Willert
Institute of Propulsion Technology ...
German Aerospace Center
51170 Koeln, Germany

ABSTRACT

We present Particle Image Velocimetry measurements in the boundary layer in turbulent Rayleigh-Bénard (RB) convection for the Rayleigh number $Ra = 1.4 \times 10^{10}$ and the Prandtl number $Pr = 0.7$. The measurements have been undertaken in a large-scale RB experiment 7.15 m in diameter and 6.30 m in height which is called the "Barrel of Ilmenau". They give detailed insight into the near-wall flow field in turbulent RB convection and provide experimental data to evaluate various competing theories on the heat transport which essentially based on the boundary layer. We found that the convective boundary layer becomes turbulent locally and temporarily although its shear Reynolds number $Re_s = U_\infty \delta/\nu \approx 265$ (U_∞ - outer velocity, δ- boundary layer thickness, ν- kinematic viscosity) is considerably smaller than the value 420 underlying existing phenomenological theories.

INTRODUCTION

Rayleigh-Bénard convection (RBC) in an infinite fluid layer heated from below and cooled from above is a canonical problem of turbulence research [Ahlers, 2009]. It represents a great variety of heat transfer problems as diverse as atmospheric and oceanic circulation, room ventilation or convection in the outer Earth's core. Although RBC has been comprehensively investigated over the past two decades, our understanding of the transition to the "ultimate regime" at very high Rayleigh numbers, $Ra = (\beta g \Delta T H^3)/(\nu\kappa)$, ($\beta$ – thermal expansion coefficient, g – gravitational acceleration, ΔT – temperature difference across the fluid layer, H – thickness of the fluid layer, ν – kinematic viscosity, κ – thermal diffusivity), is still incomplete [Kraichnan, 1962]. This is partially due to the lack of knowledge whether and under which conditions the near-wall flow field at the heating and the cooling plates (often referred to as boundary layer) undergoes a transition from laminar to turbulent flow. Although a great number of various Rayleigh-Bénard experiments exist, only a few ones meet all criteria to give insight into the structure of the near-wall flow field: i) a sufficiently high Ra number, ii) a measurement technique that resolves the near-wall flow field, iii) an accessible working fluid. Actually, there are only two facilities in the world that fulfil all requirements to measure the velocity field in the near-wall flow region with a sufficiently high resolution to discriminate between various predictions: The 81 cm by 20 cm by 76 cm water cell at The Chinese University of Hong Kong [Zhou, 2010] and the Barrel of Ilmenau, 6.30 m in height and 7.15 m in diameter in which air is used as working fluid [du Puits, 2014]. In both facilities Ra numbers up to the order of $Ra = 10^{12}$ are feasible and the spatial resolution of the velocity measurement technique used is better than one-tenth of the total boundary layer thickness. However, it is important to mention here that the Prandtl numbers differ by roughly a factor of seven (for water $Pr \approx 5$, for air $Pr = 0.7$) and, in particular, the laminar-turbulent transition of the boundary layers might be strongly affected by that difference. The aim of the work reported here is to give an insight into the boundary layer flow field in the parameter domain of Rayleigh numbers close to the transition towards the "Ultimate regime of convection". Our data clearly demonstrate that the convective layer displays features of turbulence significantly below the expected threshold of $Re_s = U_\infty \delta/\nu = 420$.

EXPERIMENTAL SET-UP

The measurements have been undertaken in a large-scale RB experiment, the "Barrel of Ilmenau". This RB cell with a diameter of $D = 7.15$ m and a maximum thickness of the fluid layer of $H = 6.30$ m. It is filled with air and currently the only one where Ra numbers up to $Ra = 10^{12}$ can be set and the boundary layer is sufficiently large (of the order of 10 mm) to probe the flow field with commercial measurement techniques. The ambient air is confined between the heated bottom plate and the free-hanging cooling plate as well as a virtually adiabatic sidewall. A water circulation inside both plates makes the temperature at the surface uniform and balances the differences of the convective heat flux at the plate–air interface. The deviation of any local temperature at the surface from the global mean temperature was typically less than ±1% of the total temperature drop between the plates (±1.5% at the cooling plate). Over the period of one

measurement, the mean surface temperature varies in a band ±0.02 K. Both plates are levelled horizontally with a maximum error of 0.1° and their distance is measured with an accuracy better than 0.5 cm. In order to ensure the adiabatic boundary condition the sidewall of the cell consists of two insulating layers with an electrical panel heating system in between. The temperature of each of the 18 heating panels around the cell is controlled in such a way that the temperature of the panel is equal to the temperature at the interface between the inner insulating layer and the air. As long as the temperature inside the RB cell does not fall below the ambient temperature – a condition which was satisfied in all experiments reported here - this system effectively prevents the heat flow through the sidewall. A sketch of the facility is shown in Figure 1. A detailed description of the facility can be found in [du Puits, 2013].

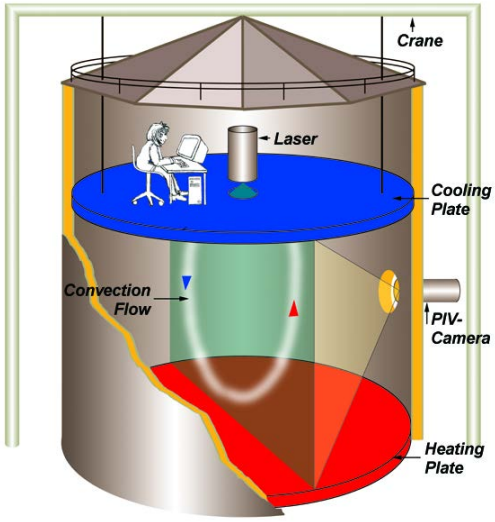

Figure 1: Sketch of the large-scale Rayleigh-Bénard experiment "Barrel of Ilmenau".

We acquired PIV data in a rectangular box of the size 2.5 × 2.5 × 0.62 m^3 (width × height × depth). The specific shape was chosen to supress the angular dynamics of the large-scale circulation and to align the laser light sheet with the plane of the wind. The box is made of transparent Perspex and was placed inside the large RB cell using its original heating and cooling plates as bottom and top walls. The temperature difference between the bottom and top wall is $\Delta T = 10$ K. In order to obtain more detailed information on the statistics and the temporal evolution of the boundary layer flow long PIV image sequences were recorded at various positions near the center line of the heated bottom plate (Fig. 2). Laser light sheet illumination was realized with a 2 W continuous wave laser. A smoke generator, based on an evaporation-condensation principle, was used to seed the flow with 1…2 µm droplets whose life time exceeded one hour.

Images of the illuminated particles were acquired with a high-speed camera (PCO GmbH, Dimax-S4) at a frame rate of 200 Hz and a spatial resolution of 2016 x 600 pixels. Aside from its high light sensitivity the main benefits of this camera is its large dynamic range of 12 bits and large internal storage to capture long sequences of more than 20,000 frames at the chosen resolution. The acquired image sequences were processed pair-wise with conventional PIV processing software (PIVTEC GmbH, PIVview2C, v3.5) using sample sizes of 24 x 16 pixels (W x H) and 64 x 8 pixels at 50 per cent overlap, where the latter sample size was chosen to improve the resolution in the presence of strong, near-wall shearing motions. Table 1 and Figure 3 provide an overview of the acquired measurement domains.

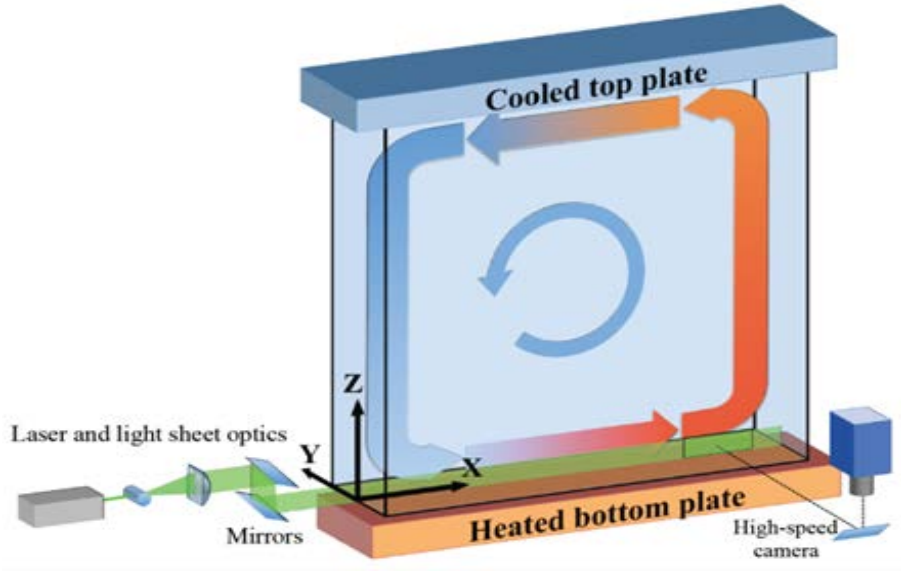

Figure 2: Setup of the PIV measurement in the rectangular box

Table 1: Imaging parameters for the acquired PIV sequences of near wall RBC

	Symbol	Overview	Detailed view A,B,C,D	Unit
Magnification	m	9.1	22.1	pixel/mm
Field of view	[W × H]	220 × 65	13 × 68	mm²
	[W × H]	2016 × 600	288 × 1500	pixel
Camera frame rate	f_{acq}	200	100/200	Hz
Camera exposure	t_{exp}	2.0	2.0	ms
Duration	t_{seq}	106	592/296	s
Number of frames	N	21,161	59,235	

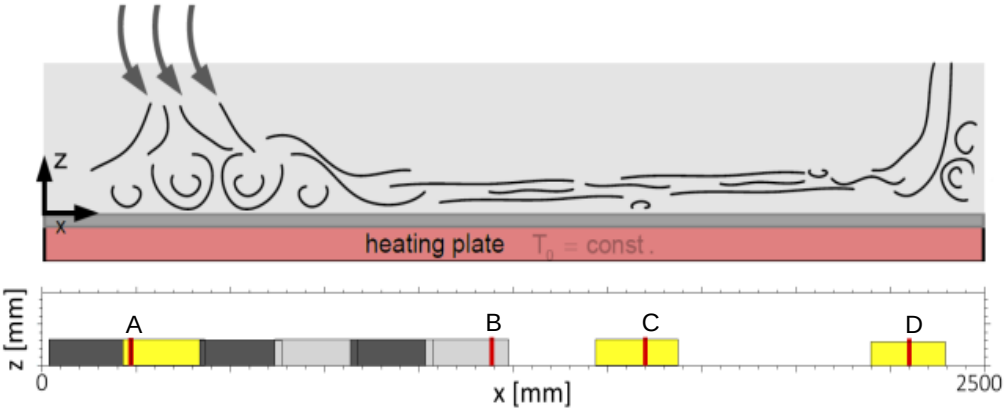

Figure 3: Schematic of the flow field (bottom plate) and overview of PIV measurement areas.

RESULTS

As sketched in Fig. 3, the flow field at the heating (cooling) plate of the rectangular RB sample can be distinguished into three various flow regions: i) the area where plumes of cooler air generated at the upper plate impinge the surface of the heating plate (left area, $0\ \text{mm} < x < 500\ \text{mm}$); ii) the area where the orientation of the flow is essentially parallel to the plate (central area, $500\ \text{mm} < x < 2000\ \text{mm}$), and iii) the area where the horizontal flow interacts with the sidewall and gets deflected upwards (right area, $2000\ \text{mm} < x < 2500\ \text{mm}$). The typical flow field in these three areas behaves completely different and is subject of the discussion in [du Puits, 2014]. That paper is complemented by supplementary video material in which typical examples of the flow field at all three positions are shown.

In our presentation we will focus on the flow field at the center positions $x = 1200$ mm (Position B in Fig. 3) and $x = 1600$ mm (Position C) As outlined in Fig. 3 the large-scale circulation shears the heating plate and a boundary layer develops in this area. A movie of the flow visualization shown during the presentation demonstrates the complexity and the dynamics of such a boundary layer in turbulent RB convection even at moderate Ra numbers as low as $Ra = 1.4 \times 10^{10}$. Through qualitative analysis (visual inspection) four characteristic flow phases could be identified:

- a laminar flow phase
- a transitional flow phase due to the inner shear and thermal instabilities within the boundary layer
- transitional flow phase due to the entrainment of coherent structures from the mean wind
- a fully turbulent flow phase

In order to give the reader of this paper an idea on the typical flow field without access to the videos two snapshots of the instantaneous velocity field along with the out-of-plane vorticity for two different flow phases are plotted in Fig. 4. In the upper sub-figure all velocity vectors are strictly aligned parallel to the plate and the vorticity field is very weak except very close to the surface where the wall-normal velocity gradient is strong. In the lower sub-figure the instantaneous flow field looks completely different. There is still a mean flow from left to right but it is superimposed by various vortical structures occurring even in the very inner part of the boundary layer. It is interesting to note that both vector plots shown in Fig. 4 are separated by only 1.7 s which is very distinctive behaviour of a transitional state towards turbulence. This intermittent behaviour was found in the entire central area ($500\ \text{mm} < x < 2000\ \text{mm}$).

The high spatial resolution of our PIV measurements also permits to analyse how this intermittency affects the profile of the mean horizontal velocity U(z) and allows to evaluate various theoretical predictions. In Fig. 5 two profiles obtained from the PIV measurements at $x = 1200$ mm (Position B in Fig. 3) and $x = 1600$ mm (Position C) are plotted along with the

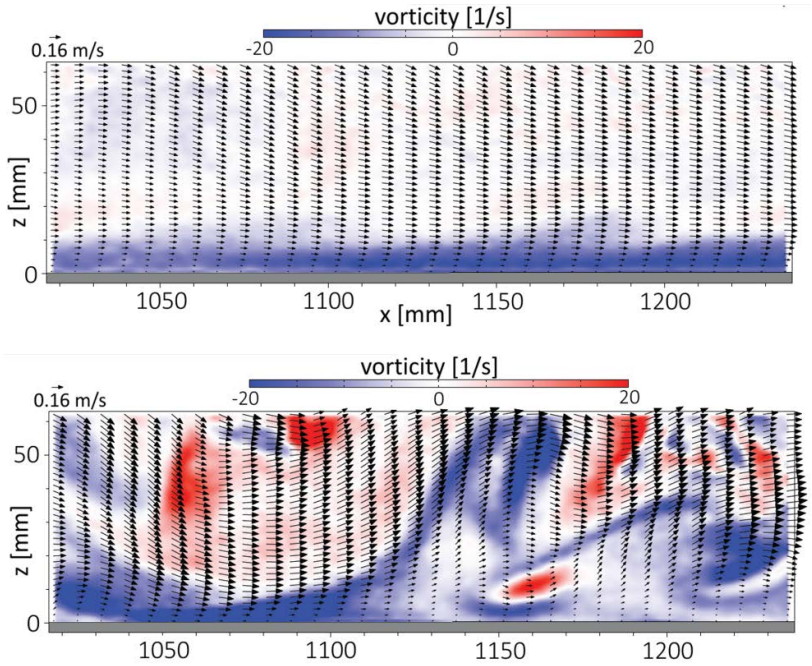

Figure 4: Two different flow phases at position $x = 1200$ mm separated by 1.7 seconds in time. Vectors are down-sampled by a factor of 8 horizontally and 2 vertically.

prediction of a pure laminar boundary layer according to Prandtl/Blasius. In order to fit the measured profiles to the prediction the mean velocity U was scaled by its maximum and the wall-normal distance z was normalized by the boundary layer thickness δ (based on U_{max}). While the measured profiles fit the laminar prediction in the very inner region of the boundary layer ($z/\delta < 0.2$), it is quite apparent that they deviate from the laminar model beyond. This is mainly caused by two reasons: i) local buoyancy effects in combination with the local shear destabilize the boundary layer, ii) coherent structures in the mean wind penetrate the boundary layer from above. Both effects gain the transition towards turbulence even though the critical shear Reynolds number $Re_s = 420$ derived from a stability analysis of an isothermal flow along a flat plate [Tollmien, 1929] is not exceeded. In particular, the second one seems to be underestimated in recent theories on the heat transport in turbulent RB convection. In order to demonstrate how these coherent structures affect the near-wall flow field we plot the correlation function between the wall-normal component of the velocity at the outer edge of the boundary layer $v(z/\delta = 1)$ and the wall shear rate which is defined as $\dot{\gamma}_w = \partial U/\partial z|_{z=0}$ in Fig. 6.

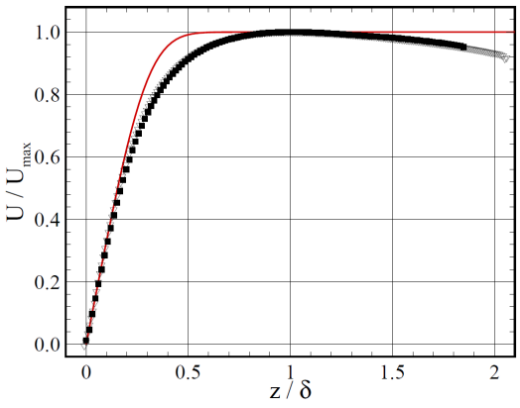

Figure 5: Wall-normal distribution of the mean horizontal velocity at $x = 1200$ mm (Position B in Fig. 3) and $x = 1600$ mm(Position C) with mean velocities of $U_{max} = 169$ mm/s and $U_{max} = 155$ mm/s. The red line is the Prandtl/Blasius prediction.

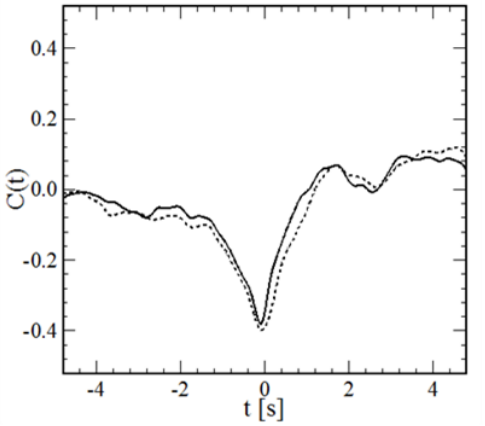

Figure 6: Cross-correlation between the wall shear rate and the wall-normal component of the velocity vector

Table 2: Boundary layer data obtained for measurement positions A through D

	Symbol	A	B	C	D	Unit
Position	x/L	0.09	0.48	0.64	0.92	-
Boundary layer thickness	δ	22.8	32.8	35.8	62.9	[mm]
Boundary layer thickness	$\delta_{99\%}$	18.7	25.3	27.7	51.3	[mm]
Kinematic boundary layer thickness	δ_v	8.05	9.82	10.9	21.6	[mm]
Displacement thickness	δ_*	5.32	6.78	7.54	14.3	[mm]
Momentum thickness	Θ	2.49	3.06	3.45	6.13	[mm]
Shape factor	$S = \delta_*/\Theta$	2.14	2.22	2.18	2.34	-
Maximum velocity	U_{max}	-37.8	169	155	83.2	[mm s^{-1}]
Wall shear rate	$\dot{\gamma}_w = dU/dz$	3.83	16.7	13.7	2.85	[s^{-1}]
Friction velocity	U_τ	7.88	16.4	14.9	6.79	[mm s^{-1}]
Wall unit	z^+/z	0.486	1.015	0.920	0.419	[mm^{-1}]
Reynolds number	Re_δ	(53)	343	343	323	-
Reynolds number	$Re_{\delta v}$	(19)	103	104	111	-
Reynolds number	$Re_{\delta *}$	(12)	71	72	73	-

There is a clear (negative) correlation between both quantities that verifies the physical relevance of the transport of bulk induced turbulence towards the inner boundary layer. Detailed PIV measurements have also been done at other x –positions along the heating plate (see Table 1) but the results will not be discussed in detail here. However, a summary of the main results is provided in Table 2.

CONCLUSIONS

The velocity field close to the bottom plate in turbulent RB convection in air has been studied experimentally using long sequences of time-resolved PIV data. It was found that even though both, Ra and shear Re numbers are below their critical thresholds of $Ra_c \approx 10^{14}$ and $Re_{s,c} = 420$, respectively, the boundary layer becomes turbulent locally and temporarily. As well inner shear and local buoyancy effects as external forcing by coherent structures from the mean wind trigger the transition of the boundary layer towards turbulence. All three contributions must be considered, when predicting the critical bound towards the so-called "ultimate regime" of thermal convection (Kraichnan, 1962).

ACKNOWLEDGEMENTS

This work was supported by the German Research Foundation under the grant numbers PU 436/3-1, PU 436/3-2 and PU 436/1-2. Major financial contribution was also provided by the European Union under the grant number 312778. Moreover, we wish to acknowledge our colleagues C. Resagk, R. Kaiser and N. Schemet for scientific discussions and V. Mitschunas and S. Abawi for their technical support to operate the facility and to run the measurements.

REFERENCES

Ahlers, G., Grossmann, S. and Lohse, D. 2009, “Heat transfer and large scale dynamics in turbulent Rayleigh-Bénard convection”, *Rev. Mod. Phys.*, Vol. 81, pp. 503.

Kraichnan, R. H. 1962, "Turbulent thermal convection at arbitrary Prandtl number", *Physics of Fluids*, Vol. 5, pp. 1374.

Zhou, Q., Xia, K.-Q. 2010, "Measured Instantaneous Viscous Boundary Layer in Turbulent Rayleigh-Bénard Convection", *Phys. Rev. Lett.*, Vol. 104, pp. 104301.

du Puits, R., Li, L., Resagk, C., Thess, A., Willert, C. 2014, “Turbulent Boundary Layer in High Rayleigh Number Convection in Air”, *Phys. Rev. Lett.*, Vol. 112, pp. 124301.

du Puits, R., Resagk, C., Thess, A. 2013, “Thermal boundary layers in turbulent Rayleigh-Bénard convection at aspect ratios between 1 and 9”, *New J. Phys.*, Vol. 15, pp. 013040.

Tollmien, W. 1929, “Über die Entstehung der Turbulenz”, *Nachr. Ges. Wiss. Goettingen, Math. Phys. Klasse*, pp. 21.